

Woolf and Salter 2000; Scholz and Woolf 2002). However, recent studies have revealed that spinal non-neuronal cells, such as microglia and astrocytes, play important roles in hypersensitivity to pain (Watkins *et al.* 2001; Scholz and Woolf 2007; Suter *et al.* 2007). From the fact that morphological activation of both microglia and astrocytes occurs relatively late after the injury, it has been speculated that the activation of these non-neuronal cells may participate in the maintenance of pain hypersensitivity (Hains and Waxman 2006; Zhuang *et al.* 2006; Tawfik *et al.* 2007; Zhao *et al.* 2007). In recent years, however, much more attention has been focused on the earlier involvement of activated microglia in neuropathic pain (Jin *et al.* 2003; Tanga *et al.* 2004; Minoru *et al.* 2006; Zhang and De Koninck 2006; Zhuang *et al.* 2007; Inoue and Tsuda 2009). Microglial activation in terms of gene transcription of CD11b, TLR4 and CD14 occurs as early as 4 h after nerve transection, while astrocyte activation was still delayed until at least day 4 post-operation (Tanga *et al.* 2004). Furthermore, there is a report that neural damage leads to rapid (within minutes) microglial activation in the central nervous system (Gehrmann *et al.* 1995). Although it remains unknown which signals initiate the activation of microglia, it is considered to be related to the injury-induced stimulation of primary afferent neurons and post-synaptic neurons. From this point of view, we have previously reported that LPA *in vitro* rapidly (within minutes to hours) activates rat microglia in primary culture, in terms of membrane 'ruffling' and brain-derived neurotrophic factor synthesis through ATP release (Fujita *et al.* 2008). In the present study, we report that microglial activation and *de novo* LPA production may play synergistic roles in the mechanisms of initiation of neuropathic pain.

Material and methods

Animals

Male C57BL/6J mice (Tagawa Experimental Animal Laboratory, Nagasaki, Japan) weighing 20–24 g were used in the present study. They were kept in a room maintained at $21 \pm 2^\circ\text{C}$ and $55 \pm 5\%$ relative humidity with a 12 h light/dark cycle, and had free access to a standard laboratory diet and tap water. The procedures were approved by the Nagasaki University Animal Care Committee, and complied with the fundamental guidelines for the proper conduct of animal experiments and related activities in academic research institutions under the jurisdiction of the Ministry of Education, Culture, Sports, Science and Technology, Japan.

Drugs

Lysophosphatidic acid (18 : 1) and minocycline were purchased from Sigma (St. Louis, MO, USA). For *in vitro* experiments, LPA was dissolved in Dulbecco's modified Eagle's medium (DMEM) containing 0.1% fatty acid-free bovine serum albumin (BSA, A-6003; Sigma-Aldrich). For *in vivo* experiments, LPA was dissolved in artificial cerebrospinal fluid (125 mM NaCl, 3.8 mM KCl, 1.2 mM KH_2PO_4 , 26 mM NaHCO_3 , 10 mM glucose).

Intrathecal injection

The i.t. injection was carried out as previously reported (Ma *et al.* 2009a), according to the modified method (Hylden and Wilcox 1980). In this method, the unanesthetized mouse was held by one hand, and the syringe was held in the other hand. The needle was inserted into the tissue between the dorsal aspects of lumbar region 5 and 6, at an angle of about 20° above the vertebral column, then was slipped into the groove between the spinous and transverse processes. Changing the angle of the syringe to 10° , the needle was carefully moved forward to the intervertebral space, and 5 μL of drug solution was injected. A reflexive flick of the tail indicated each accurate injection.

Quantitative real-time PCR

According to the described methods (Uchida *et al.* 2010a,b), at different time-points (see Results for details) after the injection of LPA, the lumbar (L4–6) SCs of control and LPA-treated mice were isolated, and lysed with TRIzol (Invitrogen, Carlsbad, CA, USA) for RNA preparation. Total RNA (1 $\mu\text{g}/\text{sample}$) was used for cDNA synthesis with PrimeScript[®] RT reagent Kit (Takara, Otsu, Japan). Quantitative real-time PCR was performed using qPCR MasterMix Plus for SYBR Green I (Eurogentec, Seraing, Belgium) with the ABI Prism 7000 sequence detection system (Applied Biosystems, Tokyo, Japan). The PCR primers used were as follows: for glyceraldehyde-3-phosphate dehydrogenase, 5'-TATGACTCCACTCACGGCAAAT-3' (forward) and 5'-GGGTCTCGCTCCTGGAA-GAT-3' (reverse); for CD11b, 5'-CTGCCTCAGGGATCCGGAA-AG-3' (forward) and 5'-TCTGTCTGCCTCGGGGATGACATC-3' (reverse). Glyceraldehyde-3-phosphate dehydrogenase was used as an internal control for normalization. In all cases, the validity of amplification was confirmed by the presence of a single peak in the melting temperature analysis and linear amplification with increasing number of PCR cycles.

Immunohistochemistry

After the defined time points, control, LPA- or injury-treated mice were deeply anesthetized by intraperitoneal (i.p.) injection of pentobarbital (50 mg/kg), and perfused with potassium-free phosphate buffered saline (K^+ -free PBS, pH 7.4), followed by 4% paraformaldehyde solution. The L4–6 SCs were isolated, post-fixed in the same fixative for 3 h, and replaced with 25% sucrose overnight. Tissues were fast-frozen in cryo-embedding compound on a mixture of ethanol and dry ice and stored at -80°C until use. The SCs were cut on a cryostat at a thickness of 20 μm and processed with 0.1% sodium azide in K^+ -free PBS. The sections were then incubated with 50% and 100% methanol for 10 min, respectively. For ionized calcium binding adaptor molecule 1 (Iba1) immunostaining, the SC sections were blocked with 2% BSA in PBST (0.1% Triton X-100 in K^+ -free PBS) for 1 h at 25°C , and incubated overnight at 4°C with anti-Iba1 antibody (anti-rabbit, 1 : 1000; Wako, Osaka, Japan). After washing, sections were incubated with secondary antibody, Alexa Fluor 594-conjugated anti-rabbit IgG (1 : 300; Invitrogen), for 3 h at 25°C .

For double immunofluorescence, the SC sections were incubated with blocking buffer containing anti-mouse IgG (1 : 50; Invitrogen) and 5% normal goat serum (Chemicon International, Temecula, CA, USA) in PBST for 2 h at 25°C , and then incubated with anti-phosphor-p38 (anti-p-p38) antibody (anti-mouse, 1 : 1000; Cell

Signaling, Beverly, MA, USA) overnight at 4°C. After washing, sections were incubated with Alexa Fluor 488-conjugated anti-mouse IgG (1 : 300; Molecular Probes, Eugene, OR, USA) secondary antibody for 2 h at 25°C. Then, sections were blocked with 2% BSA in PBST for 2 h at 25°C and incubated overnight at 4°C with anti-Iba1 antibody (anti-rabbit, 1 : 1000; Wako). After washing, sections were incubated with secondary antibody, Alexa Fluor 594-conjugated anti-rabbit IgG (1 : 300; Invitrogen), for 3 h at 25°C. The stained sections were examined with a fluorescence microscope (Keyence, Osaka, Japan).

The quantification of immunofluorescence was performed by the immunofluorescence staining intensity (Romero-Sandoval *et al.* 2008). A square with sides of 200 µm was insert into the SC (laminae I–V), and the intensity of this square was analyzed by NIH ImageJ software (National Institutes of Health, Bethesda, MD, USA).

Western blotting

Western blotting analysis for p-p38, p38 and β-tubulin (as an internal control) was performed according to the manufacturer's protocol. Total protein (30 µg) extracted from L4–6 SC was separated on an sodium dodecyl sulfate–polyacrylamide gel (12%) and transferred to Amersham Hybond™-C Extra filter (GE Healthcare, Little Chalfont, UK). The filter for p-p38 was blocked with 5% milk in Tris-buffered saline with 0.1% Tween 20 for 1 h at 25°C, while the filters for p38 and β-tubulin were blocked with 5% BSA in Tris-buffered saline with 0.1% Tween 20 for 1 h at 25°C. These filters were then incubated overnight at 4°C with primary antibodies at the following dilutions: anti-p-p38 antibody (anti-mouse, 1 : 1000; Cell Signaling), p38 (anti-rabbit, 1 : 1000; Cell Signaling) and β-tubulin (anti-rabbit, 1 : 1000; Santa Cruz Biotechnology, Santa Cruz, CA, USA). Horseradish peroxidase (HRP)-conjugated anti-mouse antibody (Invitrogen) and HRP-conjugated anti-rabbit antibody (Invitrogen) were used as the secondary antibody at a dilution of 1 : 1000. Immunoreactive bands were detected using an enhanced chemiluminescent substrate (SuperSignal® West Dura Extended Duration Substrate; Pierce Biotechnology, Rockford, IL, USA) for HRP.

Nociceptive tests

In thermal paw withdrawal tests, nociception was measured as the latency to paw withdrawal evoked by exposure to a thermal stimulus (Hargreaves *et al.* 1988; Ma *et al.* 2009a,b, 2010). Unanesthetized animals were placed in Plexiglas cages on top of a glass sheet and allowed an adaptation period of 1 h. A thermal stimulator (IITC Inc., Woodland Hills, CA, USA) was positioned under the glass sheet and the focus of the projection bulb was aimed precisely at the middle of the plantar surface of the animal. A mirror attached to the stimulator permitted visualization of the plantar surface. A cut-off time of 20 s was set to prevent tissue damage.

The paw pressure test was performed as described previously (Ma *et al.* 2009a,b, 2010). Mice were placed in a Plexiglas chamber on a 6 × 6-mm wire mesh grid floor and allowed to acclimatize for 1 h. A mechanical stimulus was then delivered to the middle of the plantar surface of the right hind-paw using a Transducer Indicator (Model 1601; IITC Inc.). The pressure required to induce a flexor response was defined as the pain threshold. All behavioral experiments were performed under double-blinded conditions.

Sample preparation from tissues

At 3 h after LPA injection or sciatic nerve injury, mice were anesthetized with pentobarbital (50 mg/kg, i.p.) as previously reported (Ma *et al.* 2009b, 2010). The bilateral or unilateral dorsal horn (laminae I–V) of the L4–6 spinal cord and L4–6 DR were then removed to enable the extraction of LPA. The average wet weights of the isolated bilateral SC and DR in each mouse were 8 and 4 mg, respectively, while weights of unilateral SC and DR were 4 and 2 mg, respectively. Following their isolation, the tissue samples were placed in 1.5-mL polypropylene tubes and homogenized by sonication in 300 µL of serum-free DMEM for approximately 30 s. To extract LPA from the homogenates using a solid-phase lipid extraction method, the samples were slowly loaded onto Oasis HLB cartridges (Millipore, Tokyo, Japan), which had been pre-conditioned with 3 mL of methanol followed by 3 mL of distilled water. The columns were then washed with 3 mL of distilled water and 1 mL of chloroform. Subsequently, LPA was eluted with 600 µL of methanol and dried with N₂ gas. The final samples were dissolved in 100 µL of DMEM and stored at –80°C until analysis.

Biological titration method

B103 cells expressing LPA₁ receptors and enhanced green fluorescent protein [B103 (+) cells] were used for quantitative measurement of LPA, according to a modified method (Inoue *et al.* 2008; Ma *et al.* 2009b, 2010) based on an earlier report (Ishii *et al.* 2000). The cells were maintained as monolayer cultures on tissue culture dishes in DMEM supplemented with 10% heat-inactivated fetal bovine serum (Gibco, Carlsbad, CA, USA), penicillin and streptomycin (final concentrations: 100 U/mL and 100 µg/mL, respectively). Cells were seeded at 2.5 × 10⁴ cells/cm² onto 8-well glass slides coated with poly-L-lysine (Sigma; final concentration, 100 mg/L) and collagen (BD Bioscience, San Jose, CA, USA; final concentration, 5 µg/cm²). The cells were then cultured in DMEM containing 10% heat-inactivated fetal bovine serum at 37°C in a 5% CO₂ atmosphere for 10 h. Subsequently, the cells were cultured in serum-starved DMEM for 15 h.

In the biological assay, a standard LPA solution or a diluted tissue sample was applied to B103 (+) cells. After incubation at 37°C for 20 min, the medium was replaced with 4% paraformaldehyde followed by incubation at 25°C for 60 min. The glass slide was then cover-slipped with Fluoromount™ (DBS, Pleasanton, CA, USA) and examined under a fluorescence microscope (Keyence). The percentage of cells exhibiting a rounded morphology among at least 500 cells in each well was determined.

Phospholipase A₂ activity assays

The activities of cytosolic phospholipase A₂ (cPLA₂) and calcium-independent phospholipase A₂ (iPLA₂) were detected using the following assays as described previously (Smani *et al.* 2003; Ma *et al.* 2010). Briefly, at different time points after LPA injection or sciatic nerve injury, mice were anesthetized with pentobarbital (50 mg/kg, i.p.), and the bilateral or ipsilateral side of the SC was removed. After sonication and centrifugation at 20 000 g for 20 min at 4°C, the supernatant was collected and kept on ice. The protein concentration of the supernatant was determined by the Lowry method, and the assays were performed on the same day using a cPLA₂ assay kit (Cayman Chemicals, Ann Arbor, MI, USA) to evaluate the cPLA₂ activity or a modified cPLA₂ assay kit (Cayman

Chemicals) to evaluate the iPLA₂ activity, as described previously (Smani *et al.* 2003). In the cPLA₂ assay, the tissue samples were incubated with both bromoenol lactone, an iPLA₂ inhibitor (Ackermann *et al.* 1995), and a substrate, arachidonoyl thio-phosphatidylcholine (PC), at 20°C for 1 h in a assay buffer. The reactions were stopped by the addition of a mixture of 25 mM 5,5'-dithiobis-(2-nitrobenzoic acid) and 475 mM EGTA in 0.5 M Tris-HCl (pH 8.0) for 5 min, and the absorbances were determined at 405 nm using a standard plate reader (PerkinElmer Japan Co., Ltd, Yokohama, Japan). To detect the activity of iPLA₂, but not cPLA₂, the samples were incubated with the substrate, arachidonoyl thio-PC, at 20°C for 1 h in a modified Ca²⁺-free buffer (4 mM EGTA, 160 mM HEPES pH 7.4, 300 mM NaCl, 8 mM Triton X-100, 60% glycerol, 2 mg/mL of BSA). The reactions were stopped by the addition of 5,5'-dithiobis-(2-nitrobenzoic acid) for 5 min. The activity of PLA₂ was defined as the percentage of the control activity as follows: LPA- or injury-treated tissues (absorbance/mg of protein)/normal tissues (absorbance/mg of protein) × 100.

Partial sciatic nerve ligation

Partial ligation of the sciatic nerves was performed under anesthesia with pentobarbital (50 mg/kg, i.p.), according to modified methods (Rashid *et al.* 2003; Ma *et al.* 2009a, 2010). The common sciatic nerve of the right hind limb was exposed at the high thigh level through a small incision and the dorsal half of the nerve thickness was tightly ligated with a silk suture. A sham-operation was performed similarly except without touching the sciatic nerve.

Minocycline treatment

Generally, early treatment with minocycline (10 or 30 mg/kg, i.p.) involved daily injection from 1 day before LPA/injury to day 2 after LPA/injury treatment, while late treatment with minocycline (30 mg/kg, i.p.) was performed daily from day 2 to day 5 after LPA/injury treatment. In the experiments measuring LPA-induced increases in expression of CD11b and p-p38 at day 1 post-LPA-treatment, minocycline was injected daily from 1 day before LPA to day 1 after LPA treatment. In the experiments measuring *de novo* LPA production and PLA₂ activities, on the other hand, minocycline was injected at 1 day before and at 30 min before LPA- or nerve injury-treatment.

Statistical analysis

Statistical analyses were carried out using Student's *t*-test and Tukey's multiple comparison *post hoc* analysis following one-way ANOVA. The criterion of significance was set at $p < 0.05$. All results are expressed as means ± SEM.

Results

Minocycline-reversible LPA-induced microglial activation

In response to various stimuli, microglia rapidly increase the expression of various surface antigens (Rock *et al.* 2004). Among the different surface markers, CD11b, a member of the β2 integrin family, is potentially the one with the most biological significance (Ling and Wong 1993; Rock *et al.* 2004; Roy *et al.* 2006). CD11b is detectable in resting microglia, and its expression at the mRNA or

protein level is greatly increased in active microglia (González-Scarano and Baltuch 1999; Tanga *et al.* 2004; Roy *et al.* 2006).

As shown in Fig. 1(a), quantitative real-time PCR showed that the LPA (1 nmol, i.t.)-induced increase in CD11b mRNA levels in SC started as early as 3 h, and a significant increase was observed at 12 h and day 1 after LPA injection. The increase was then followed by a gradual decline by day 7 after LPA treatment. Minocycline, a microglial activation inhibitor (Tikka and Koistinaho 2001; Tikka *et al.* 2001), was used in this study. Three early treatments with minocycline (30 mg/kg, i.p.) at -1, 0 and 1 day after LPA injection significantly reversed the increased CD11b mRNA expression observed at day 1, but did not affect the basal levels (Fig. 1a).

As Iba1 is specifically up-regulated in activated microglia and mediates the morphological changes of microglia (Ito *et al.* 1998), we evaluated the microglial activation by measuring LPA-induced Iba1-immunoreactivity. At day 1 after LPA (1 nmol, i.t.) injection, we observed a significant increase in the intensity of Iba1-immunoreactive cells, accompanied by a dramatic change in morphology from the ramified to the amoeboid type. These changes reached a maximum at day 3, and had then declined by day 7 (Fig. 1b-g), which was consistent with CD11b gene expression. However, early treatments with minocycline (30 mg/kg, i.p.), at -1, 0, 1 and 2 days after LPA injection significantly inhibited the microglial activation, in terms of the increased intensity and morphological changes (Fig. 1f and g).

Minocycline-reversible p38 activation

It is well-known that p38, a member of the family of mitogen-activated protein kinases, is predominantly activated in microglia in the spinal cord under various pain conditions, and participates in the initiation and development of pain hypersensitivity (Kim *et al.* 2002; Jin *et al.* 2003; Piao *et al.* 2006). Therefore, activated (phosphorylated) p38 (p-p38) can serve as a functional marker for microglial activation (Jin *et al.* 2003; Romero-Sandoval *et al.* 2008). In this study, to verify the location of p-p38, double immunostaining study of p-p38 and Iba1 was performed. It was found that p-p38 is completely co-localized with Iba1 in SC at day 3 after LPA injection (Fig. 2a-c). Further, the early treatments with minocycline (30 mg/kg, i.p.) significantly reversed the expression of p-p38 and Iba1 (Fig. 2d-f).

In addition, western blot was performed to evaluate the time-dependent changes of p38 activation after LPA (1 nmol, i.t.) injection. As shown in Fig. 2(g and h), there was an increase in p-p38 protein levels at 3 and 12 h after LPA treatment in SC. This increase was significantly detectable at day 1 and 3 after LPA injection, and was attenuated at day 7 (Fig. 2i and j), consistent with CD11b and Iba1 expression. Early treatments with minocycline (30 mg/kg, i.p.) significantly blocked the up-regulation of p-p38 levels at day 1 and

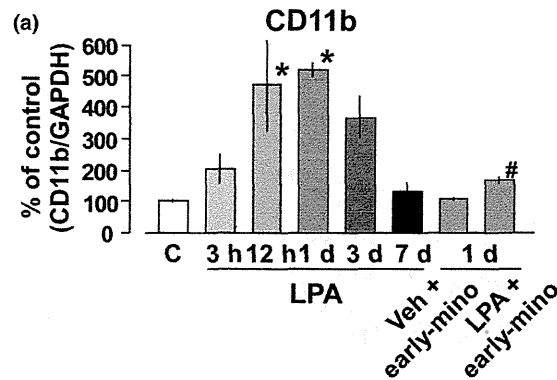
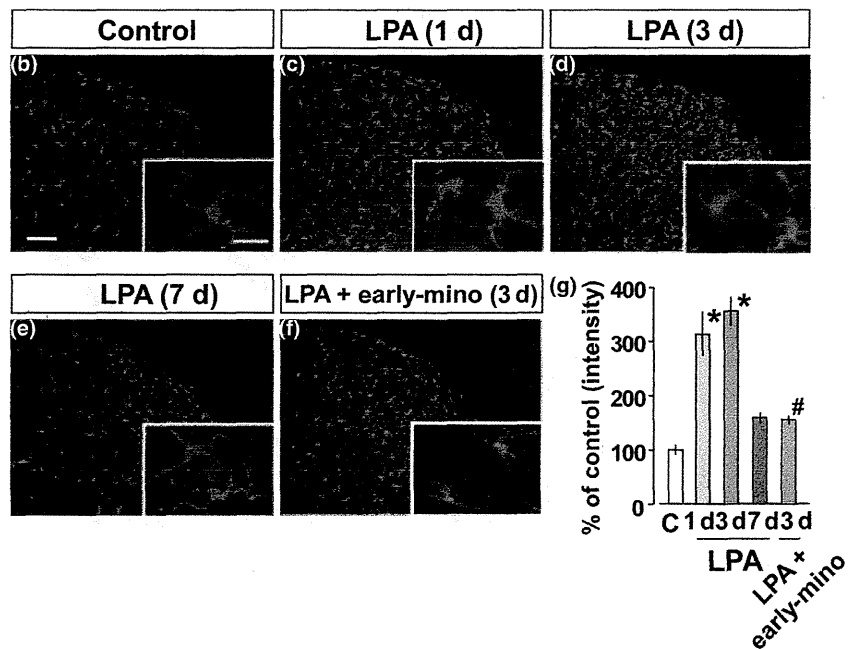


Fig. 1 Minocycline-reversible LPA-induced microglial activation. (a) Time course of CD11b mRNA expression in the spinal dorsal horn (SC) after treatment with LPA alone or minocycline plus LPA, assessed using quantitative real-time PCR. (b–f) Time course of Iba1 expression in the SC after treatment with LPA alone or minocycline plus LPA, assessed using immunohistochemistry. Scale bar (low magnification), 100 μ m; Scale bar (high magnification), 20 μ m. (g) Quantification of Iba1 expression by immunofluorescence staining intensity. The data were expressed as the intensity per square 200 μ m and represent five slices per group. The capital letter 'C' represents the control group (naive mice). The 'mino' represents minocycline. All data represent means \pm SEM from three or four mice. * p < 0.05, versus the control group; # p < 0.05, versus the LPA-treatment group at day 1 (a) or day 3 (g).



3 after LPA injection (Fig. 2g–j). The total non-phosphorylated p38 levels did not change during this time (Fig. 2g–j).

Early treatments with minocycline reversed LPA-induced neuropathic pain

We previously demonstrated that a single LPA (1 nmol, i.t.) injection caused robust thermal hyperalgesia and mechanical allodynia (Inoue *et al.* 2004). In this study, we found that daily treatments with minocycline (30 mg/kg, i.p.), at –1 to 2 days after LPA injection, abolished the LPA-induced neuropathic pain-like behavior, but did not affect the nociceptive thresholds in vehicle-treated mice (Fig. 3a and b). On the other hand, the later treatments with minocycline (30 mg/kg, i.p.) at 2–5 days after LPA injection had no effect on the behavioral changes (Fig. 3c and d). Quantitative comparison of nociception levels was demonstrated by the area under the curve of nociception, as shown in Fig. 3(e and f). The complete blockade of LPA-induced neuropathic pain-like behavior was observed using minocycline at 30, but not 10 mg/kg.

Minocycline reverses LPA-induced enhancement of *de novo* LPA production and cPLA₂ activity

We previously found that a single LPA (1 nmol, i.t.) injection caused feed-forward *de novo* LPA production in the SC and DR (Ma *et al.* 2009b). To investigate the role of microglial activation in this LPA production, we performed two early treatments with minocycline (30 mg/kg, i.p.), at 1 day before and 30 min before LPA treatment, and found that minocycline significantly blocked *de novo* LPA production in the SC and DR at 3 h after LPA injection (Fig. 4a and b).

For the study of the signal transduction pathway leading to LPA production, we measured the enzymatic activities of cPLA₂ and iPLA₂, which are expressed in the spinal cord (Karin Killermann *et al.* 2005) and catalyze PC conversion to lysophosphatidylcholine (LPC) (Aoki 2004; Aoki *et al.* 2008; Inoue *et al.* 2008). Furthermore, we recently reported that nerve injury remarkably increases the activities of cPLA₂ and iPLA₂ within hours (Ma *et al.* 2010). As shown in Fig. 4(c), there was some increase in activity of both cPLA₂ and iPLA₂ at 1 h after LPA treatment, while a significant

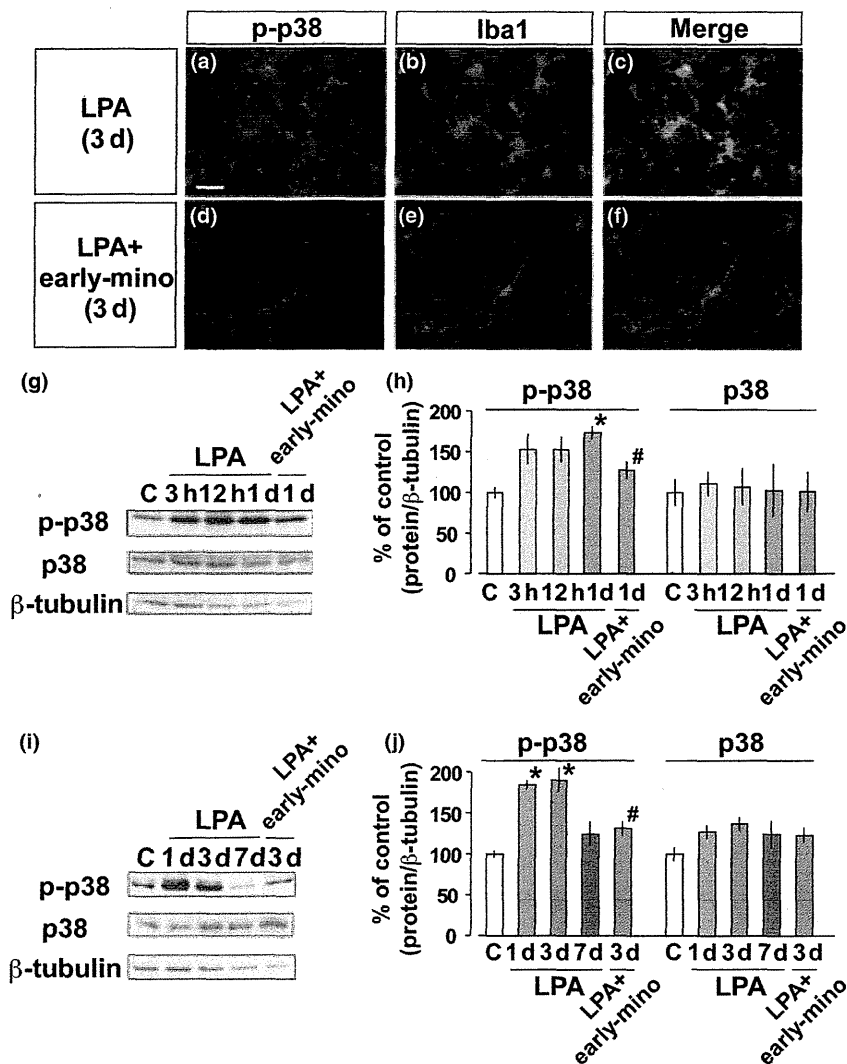


Fig. 2 Minocycline-reversible p38 activation. (a–f) Immunohistochemical double labeling of p-p38 (green) and Iba1 (red) in the SC after treatment with LPA alone or minocycline plus LPA. (g and i) Time course of p-p38 and total p38 protein expression in the SC after treatment with LPA alone or minocycline plus LPA, assessed by western blot analysis. (h and j) Quantification of p-p38 and total p38 protein expression by western blot. The capital letter 'C' represents the control group (naive mice). All data represent means \pm SEM from three mice. * $p < 0.05$, versus the control group; # $p < 0.05$, versus the LPA-treatment group at day 1 (h) or day 3 (j).

increase in cPLA₂ activity was observed in the SC at 3 h. The increase then declined at 5 h after LPA treatment, this being consistent with the LPA-induced *de novo* LPA production. The increased cPLA₂ activity was also abolished by the early treatments with minocycline (Fig. 4d).

Blockade of nerve injury-induced neuropathic pain and the underlying mechanisms by early treatments with minocycline

As *i.t.* injection of LPA was found to cause the same behavioral and biochemical changes as those evoked by nerve injury (Inoue *et al.* 2004), we examined the effects of minocycline on the nerve injury-induced neuropathic pain and its underlying mechanisms. As shown in Fig. 5(a–d), early, but not late treatments with minocycline (30 mg/kg, *i.p.*) significantly inhibited nerve injury-induced neuropathic pain. Similarly, the early treatments with minocycline suppressed the nerve injury-induced microglial activation at day 3 post-injury (Fig. 5e, f and g), *de novo* LPA production in SC

and DR at 3 h after injury (Fig. 5h), and increased activities of cPLA₂ as well as iPLA₂ at 1 h after injury (Fig. 5i).

Discussion

Here, we have demonstrated for the first time that the early phase of microglial activation contributes to LPA- or nerve injury-induced neuropathic pain and its underlying mechanisms, such as *de novo* LPA production and increased PLA₂ activity. Previous studies examining the mechanisms of pain focused primarily on the neuronal plasticity (Ji *et al.* 1999; Woolf and Salter 2000; Scholz and Woolf 2002). There is, however, growing evidence that non-neuronal cells such as microglia and astrocytes also contribute to chronic pain (Watkins *et al.* 2001; Scholz and Woolf 2007; Suter *et al.* 2007). In particular, a role of microglial activation in development of pain hypersensitivity has been proposed, though the mechanism remains controversial (Jin *et al.* 2003; Tanga *et al.* 2004; Zhuang *et al.* 2007).

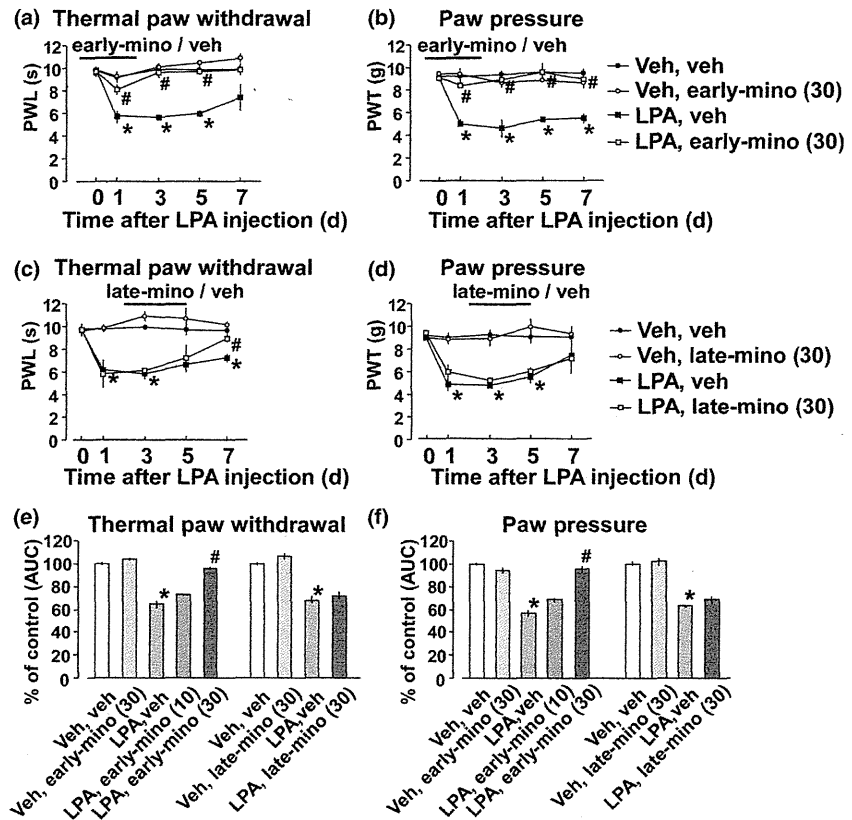


Fig. 3 Early treatments with minocycline reverse the LPA-induced neuropathic pain. (a and b) Minocycline (10 and 30 mg/kg, i.p.) was injected daily at -1, 0, 1 and 2 days after LPA treatment, and the thermal withdrawal test (*panel a*) and paw pressure test (*panel b*) were performed at the indicated time points. (c and d) Minocycline (30 mg/kg, i.p.) was injected daily from day 2 to 5 after LPA treatment, and the thermal withdrawal test (*panel c*) and paw pressure test (*panel d*) were performed at the indicated time points. (e and f) Quantification of time course thresholds for the thermal withdrawal test (*panel e*) and paw pressure test (*panel f*) in terms of the area under the curve (AUC). PWL, paw withdrawal latency; PWT, paw withdrawal threshold. All data represent means \pm SEM from three or four mice. * $p < 0.05$, versus the vehicle-vehicle group; # $p < 0.05$, versus the LPA-vehicle group.

Microglia are known to express LPA₁ and LPA₃ receptors (Moller *et al.* 2001). In microglia, several LPA-induced cellular actions have been reported such as proliferation, migration and membrane hyperpolarization (Moller *et al.* 2001; Schilling *et al.* 2002, 2004). In addition, we previously demonstrated that the cultured microglia were activated *in vitro* by LPA, in terms of membrane ruffling and brain-derived neurotrophic factor expression through ATP release (Fujita *et al.* 2008). In this study, we confirmed that the spinal microglia were rapidly activated (within as little as 3 h) by a single i.t. injection of LPA, in terms of up-regulation of CD11b mRNA, p-p38 protein levels and morphological changes in microglia, preceding the morphological change in Iba1-immunoreactive cells from ramified to amoeboid at day 1. Recent studies have reported that the phosphorylation of p38 is the upstream signal for CD11b gene transcription (Ji and Suter 2007), which is consistent with the results of our present study, in which p-p38 levels at 3 h were largely equivalent to those at 12 h, while CD11b mRNA levels at 3 h were much lower than those at 12 h. On the other hand, the up-regulation of CD11b transcription declined as early as day 3, while the decline of p-p38 levels occurred at day 7. Similar results were also observed with regard to the morphological changes, which reached a maximum at day 3 and had largely disappeared by day 7, suggesting that LPA-induced functional microglial activation precedes the morphological change.

Given that minocycline, a tetracycline-like antibiotic, has been confirmed to be a specific microglial activation inhibitor (Tikka and Koistinaho 2001; Tikka *et al.* 2001), it was used in this study to investigate whether spinal cord microglia may participate in neuropathic pain and underlying mechanisms. In the behavioral tests, LPA injection induced robust neuropathic pain-like behavior such as thermal hyperalgesia and mechanical allodynia, as previously reported (Inoue *et al.* 2004). The LPA-induced hyperalgesia and allodynia were completely suppressed when minocycline was given at the early time points of -1, 0, 1 and 2 days after the LPA injection, this being consistent with the inhibition of LPA-induced microglial activation by minocycline. However, the pain-related behavior was not affected when minocycline was given at the later time points of 2, 3, 4 and 5 days after the LPA injection, though both functional and morphological activation of microglia were still observed at the day 3 time point. Similar results were also observed in the case of nerve injury, in which neuropathic pain was abolished by the earlier, but not later treatments with minocycline, this being consistent with the previous study (Raghavendra *et al.* 2003). These findings suggest that the early stage of microglial activation may have crucial roles in the development of LPA- or nerve injury-induced neuropathic pain.

Although it remains to be determined why the later treatments with minocycline had no effect on the neuropathic pain, it may be related to the involvement of the so-called

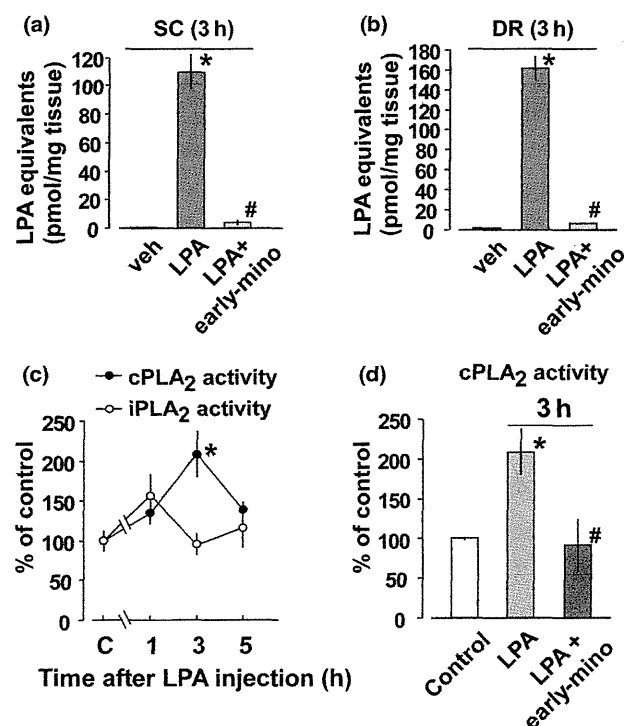


Fig. 4 Minocycline-reversible LPA-induced enhancement of *de novo* LPA production and cPLA₂ activity. (a and b) Evaluation of LPA production in the SC (panel a) and DR (panel b) at 3 h after treatment with LPA alone or minocycline plus LPA. The LPA measurements were carried out in triplicate for each sample. Cell-rounding morphology was evaluated in at least 500 enhanced green fluorescent protein-positive cells. (c) Activities of cPLA₂ and iPLA₂ in the SC after LPA (1 nmol, i.t.) injection through cPLA₂ and iPLA₂ activity assays. The capital letter 'C' represents the control group (naive mice). Specifically, the values of cPLA₂ and iPLA₂ activities in control groups are $100 \pm 1.62\%$ and $100 \pm 12.87\%$ (2.0 ± 0.4 and 2.8 ± 0.4 nmol/min/mL), respectively. (d) The minocycline-induced inhibition of cPLA₂ activity at 3 h after LPA injection. All data represent means \pm SEM from three separate experiments. * $p < 0.05$, versus the control group; # $p < 0.05$, versus the LPA group.

cytokine network between microglia and astrocytes. It is well known that microglial activation in chronic pain states stimulates the release of some proinflammatory cytokines, such as interleukin-1 β , interleukin-6 and tumor necrosis factor- α (Ji and Suter 2007; Scholz and Woolf 2007; Suter *et al.* 2007; Milligan and Watkins 2009). Accumulating reports have indicated that the proinflammatory cytokines activate astrocytes, which are involved in the maintenance of the late stage of neuropathic pain (Ji *et al.* 2009; Milligan and Watkins 2009; Gao and Ji 2010; Gao *et al.* 2010). As minocycline has no direct action on astrocytes or neurons (Yrjänheikki *et al.* 1998; Tikka and Koistinaho 2001; Tikka *et al.* 2001; Wu *et al.* 2002), the astrocyte activation may be related to the mechanisms underlying the late stage of neuropathic pain in the presence of minocycline.

Previously, we have firstly found that LPA was the initiator of nerve injury-induced neuropathic pain, which was abolished in mice lacking the LPA₁ receptor gene (Inoue *et al.* 2004). However, the basal nociceptive thresholds were not affected in these LPA₁ receptor gene homozygous mutant mice (Inoue *et al.* 2004). Moreover, the early treatments (1 h post-injury) with inhibitors of cPLA₂ and iPLA₂, which play key roles in the LPA production, significantly blocked the nerve injury-induced neuropathic pain, whereas either inhibitor had no effect on the neuropathic pain when given late (6 h post-injury) (Ma *et al.* 2010). From these findings, it seems that nerve injury-induced neuropathic pain is initiated by *de novo* biosynthesis of LPA. Indeed, we have recently demonstrated that LPA- or nerve injury-induced *de novo* LPA production in the SC and DR *in vivo* (Ma *et al.* 2009b, 2010). The peak LPA-production time after treatment in both cases was 3 h, the time when microglial activation has already started in terms of CD11b mRNA expression and p38 phosphorylation, as shown in Figs 1(a) and 2. In the present study, the LPA- or nerve injury-induced *de novo* LPA production in the SC and DR were completely inhibited by the early treatments with minocycline. Therefore, it is evident that LPA- or nerve injury-induced microglial activation is also involved in the feed-forward system through LPA production. Recent studies have revealed that LPA is produced through an ATX-mediated conversion of LPC in the central nervous system as well as peripheral tissues (Aoki 2004; Aoki *et al.* 2008; Inoue *et al.* 2008). Our previous study revealed that the intense stimulation of spinal cord slices with capsaicin or a combination of substance P and NMDA caused a synthesis of LPC, which in turn is converted to LPA in the presence of recombinant ATX. In this study, cPLA₂ or iPLA₂ inhibitor abolished the LPA synthesis in the presence of ATX (Inoue *et al.* 2008). Further study revealed that both inhibitors also blocked the nerve injury-induced *de novo* LPA production *in vivo* (Ma *et al.* 2010). Moreover, the activities of cPLA₂ and iPLA₂ are found to be elevated after nerve injury (Ma *et al.* 2010). Consistent with these previous findings, there was some, albeit non-significant, elevation of cPLA₂ and iPLA₂ activities at 1 h after LPA treatment. Significant elevation of cPLA₂ activity was observed at 3 h (Fig. 4c), and this LPA-induced elevation was abolished by the pre-treatments with minocycline. Similar results were also observed in the case of nerve injury, in which minocycline abolished the elevation of both cPLA₂ and iPLA₂ activities. Therefore, it is evident that LPA-mediated microglial activation may cause an increase in the *de novo* LPA production in terms of PLA₂ activities.

However, it remains to be determined which cell types are responsible for the source of LPA- or nerve injury-induced *de novo* LPA production. As there are reports that LPA

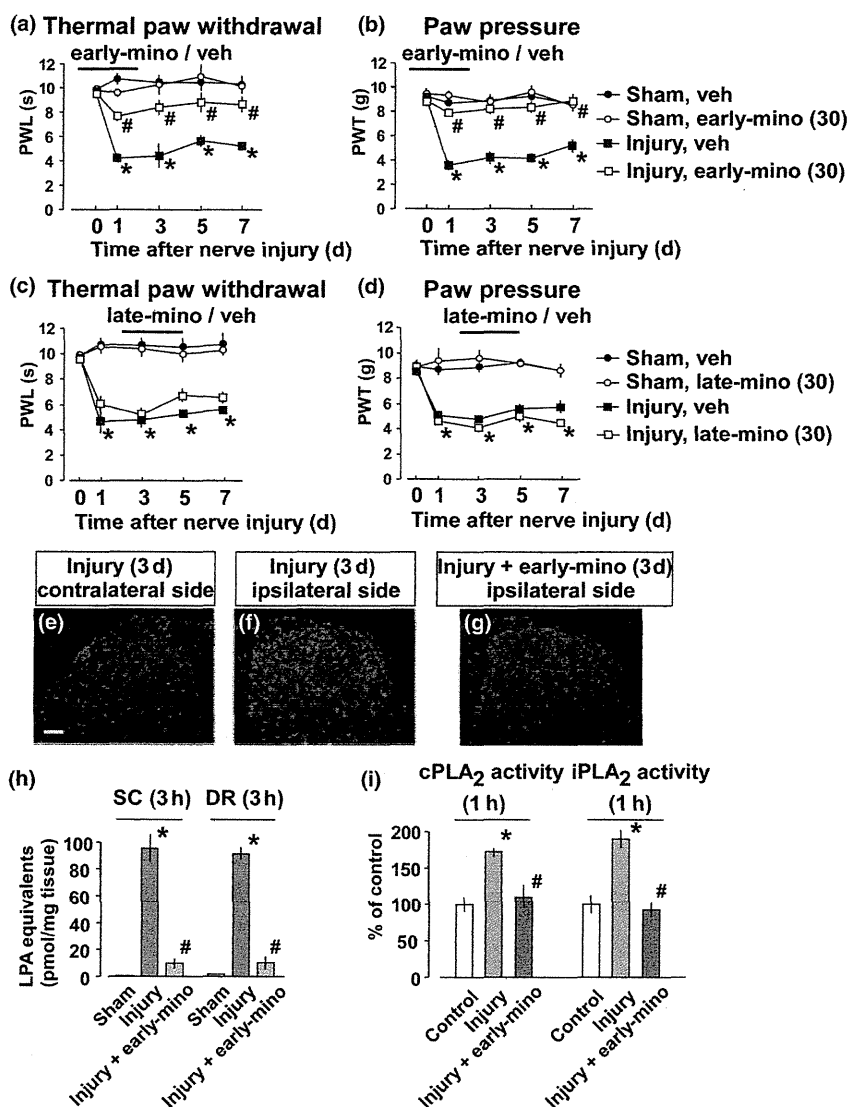


Fig. 5 Blockade of nerve injury-induced neuropathic pain and its underlying mechanisms by early treatments with minocycline. (a and b) Minocycline (30 mg/kg, i.p.) was injected daily at -1 , 0, 1 and 2 days after injury, and the thermal withdrawal test (*panel a*) and paw pressure test (*panel b*) were performed at the indicated time points. (c and d) Minocycline (30 mg/kg, i.p.) was injected daily from day 2 to 5 after injury, and the thermal withdrawal test (*panel c*) and paw pressure test (*panel d*) were performed at the indicated time points. All data were from three or four mice per group. (e–g) Immunohistochemical labeling for Iba1 at day 3 after treatment with injury alone

(*panel e and f*) or minocycline plus injury (*panel g*). Scale bar 100 μ m. (h) Evaluation of LPA production in the SC and DR at 3 h after treatment with injury alone or minocycline plus injury. The LPA measurements were carried out in triplicate for each sample. Cell-rounding morphology was evaluated in at least 500 enhanced green fluorescent protein-positive cells. (i) Activities of cPLA₂ and iPLA₂ in the SC at 1 h after treatment with injury alone or minocycline plus injury. All data represent means \pm SEM from three separate experiments. * $p < 0.05$, versus the sham-vehicle (a–d) or sham (h) or control (i) group; # $p < 0.05$, versus the injury-vehicle (a and b) or injury (h and i) group.

can be synthesized and secreted by primary neurons *in vitro* (Fukushima *et al.* 2000), and cPLA₂ and iPLA₂ are predominantly expressed in neurons (Kishimoto *et al.* 1999; Kurusu *et al.* 2008), neurons seem to be the major candidate. From the fact that minocycline abolished all these mechanisms, it is suggested that the so-called neuron-glia network may be responsible for LPA- or nerve injury-induced *de novo* LPA production and neuropathic pain. Elucidation of the

detailed mechanisms underlying the neuron-glia network would then be the next topic for investigation.

In conclusion, the results of the present study demonstrate that microglial activation is responsible for the *de novo* biosynthesis of LPA and neuropathic pain after LPA injection or nerve injury. Specifically, the early stage of microglial activation seems to be the more important mechanism and phase underlying the development of neuropathic pain.

Acknowledgements

We thank Takuya Sakurai, Tomoyo Ogawa and Sebok Kumar Halder for technical assistance. We also thank Nobuyuki Fukushima for providing the B103 cells expressing the LPA₁ receptor. This study was supported by Special Coordination Funds from the Science and Technology Agency of the Japanese Government, Grants-in-Aid from the Ministry of Education, Science, Culture and Sports of Japan and the Human Frontier Science Program, and Health Labour Sciences Research Grants from the Ministry of Health, Labour and Welfare of Japan (to Hiroshi Ueda): 'Research on Allergic Disease and Immunology' and 'Third Term Comprehensive Control Research for Cancer (398-49).'

References

- Ackermann E. J., Conde-Frieboes K. and Dennis E. A. (1995) Inhibition of macrophage Ca-independent phospholipase A by bromoenol lactone and trifluoromethyl ketones. *J. Biol. Chem.* **270**, 445–450.
- Aoki J. (2004) Mechanisms of lysophosphatidic acid production. *Semin. Cell Dev. Biol.* **15**, 477–489.
- Aoki J., Inoue A. and Okudaira S. (2008) Two pathways for lysophosphatidic acid production. *Biochim. Biophys. Acta* **1781**, 513–518.
- Fujita R., Ma Y. and Ueda H. (2008) Lysophosphatidic acid-induced membrane ruffling and brain-derived neurotrophic factor gene expression are mediated by ATP release in primary microglia. *J. Neurochem.* **107**, 152–160.
- Fukushima N., Weiner J. A. and Chun J. (2000) Lysophosphatidic acid (LPA) is a novel extracellular regulator of cortical neuroblast morphology. *Dev. Biol.* **228**, 6–18.
- Gao Y. J. and Ji R. R. (2010) Chemokines, neuronal-glia interactions, and central processing of neuropathic pain. *Pharmacol. Ther.* **126**, 56–68.
- Gao Y. J., Xu Z. Z., Liu Y. C., Wen Y. R., Decosterd I. and Ji R. R. (2010) The c-Jun N-terminal kinase 1 (JNK1) in spinal astrocytes is required for the maintenance of bilateral mechanical allodynia under a persistent inflammatory pain condition. *Pain* **148**, 309–319.
- Gehrmann J., Banati R. B., Wiessner C., Hossmann K. A. and Kreutzberg G. W. (1995) Reactive microglia in cerebral ischaemia: an early mediator of tissue damage? *Neuropathol. Appl. Neurobiol.* **21**, 277–289.
- González-Scarano F. and Baltuch G. (1999) Microglia as mediators of inflammatory and degenerative diseases. *Annu. Rev. Neurosci.* **22**, 219–240.
- Hains B. C. and Waxman S. G. (2006) Activated microglia contribute to the maintenance of chronic pain after spinal cord injury. *J. Neurosci.* **26**, 4308–4317.
- Hargreaves K., Dubner R., Brown F., Flores C. and Joris J. (1988) A new and sensitive method for measuring thermal nociception in cutaneous hyperalgesia. *Pain* **32**, 77–88.
- Hylden J. L. and Wilcox G. L. (1980) Intrathecal morphine in mice: a new technique. *Eur. J. Pharmacol.* **67**, 313–316.
- Inoue K. and Tsuda M. (2009) Microglia and neuropathic pain. *Glia* **57**, 1469–1479.
- Inoue M., Rashid M. H., Fujita R., Contos J. J., Chun J. and Ueda H. (2004) Initiation of neuropathic pain requires lysophosphatidic acid receptor signaling. *Nat. Med.* **10**, 712–718.
- Inoue M., Ma L., Aoki J. and Ueda H. (2008) Simultaneous stimulation of spinal NK1 and NMDA receptors produces LPC which undergoes ATX-mediated conversion to LPA, an initiator of neuropathic pain. *J. Neurochem.* **107**, 1556–1565.
- Ishii I., Contos J. J., Fukushima N. and Chun J. (2000) Functional comparisons of the lysophosphatidic acid receptors, LP(A1)/VZG-1/EDG-2, LP(A2)/EDG-4, and LP(A3)/EDG-7 in neuronal cell lines using a retrovirus expression system. *Mol. Pharmacol.* **58**, 895–902.
- Ito D., Imai Y., Ohsawa K., Nakajima K., Fukuuchi Y. and Kohsaka S. (1998) Microglia-specific localisation of a novel calcium binding protein, Iba1. *Mol. Brain Res.* **57**, 1–9.
- Ji R. R. and Suter M. R. (2007) p38 MAPK, microglial signaling, and neuropathic pain. *Mol. Pain* **3**, 33.
- Ji R. R., Baba H., Brenner G. J. and Woolf C. J. (1999) Nociceptive-specific activation of ERK in spinal neurons contributes to pain hypersensitivity. *Nat. Neurosci.* **2**, 1114–1119.
- Ji R.-R., Xu Z.-Z., Wang X. and Lo E. H. (2009) Matrix metalloprotease regulation of neuropathic pain. *Trends Pharmacol. Sci.* **30**, 336–340.
- Jin S. X., Zhuang Z. Y., Woolf C. J. and Ji R. R. (2003) p38 mitogen-activated protein kinase is activated after a spinal nerve ligation in spinal cord microglia and dorsal root ganglion neurons and contributes to the generation of neuropathic pain. *J. Neurosci.* **23**, 4017–4022.
- Karin Killermann L., Camilla I. S., Xiao-Ying H., Tony L. Y. and Edward A. D. (2005) Spinal phospholipase A₂ in inflammatory hyperalgesia: role of Group IVA cPLA₂. *Br. J. Pharmacol.* **144**, 940–952.
- Kim S.-Y., Bae J.-C., Kim J.-Y., Lee H.-L., Lee K.-M., Kim D.-S. and Cho H.-J. (2002) Activation of p38 MAPK in the rat dorsal root ganglia and spinal cord following peripheral inflammation and nerve injury. *NeuroReport* **13**, 2483–2486.
- Kishimoto K., Matsumura K., Kataoka Y., Morii H. and Watanabe Y. (1999) Localization of cytosolic phospholipase A2 messenger RNA mainly in neurons in the rat brain. *Neuroscience* **92**, 1061–1077.
- Kurusu S., Matsui K., Watanabe T., Tsunou T. and Kawaminami M. (2008) The cytotoxic effect of bromoenol lactone, a calcium-independent phospholipase A2 inhibitor, on rat cortical neurons in culture. *Cell. Mol. Neurobiol.* **28**, 1109–1118.
- Ling E. A. and Wong W. C. (1993) The origin and nature of ramified and amoeboid microglia: a historical review and current concepts. *Glia* **7**, 9–18.
- Ma L., Matsumoto M., Xie W., Inoue M. and Ueda H. (2009a) Evidence for lysophosphatidic acid 1 receptor signaling in the early phase of neuropathic pain mechanisms in experiments using Ki-16425, a lysophosphatidic acid 1 receptor antagonist. *J. Neurochem.* **109**, 603–610.
- Ma L., Uchida H., Nagai J., Inoue M., Chun J., Aoki J. and Ueda H. (2009b) Lysophosphatidic acid-3 receptor-mediated feed-forward production of lysophosphatidic acid: an initiator of nerve injury-induced neuropathic pain. *Mol. Pain* **5**, 64.
- Ma L., Uchida H., Nagai J., Inoue M., Aoki J. and Ueda H. (2010) Evidence for de novo synthesis of lysophosphatidic acid in the spinal cord through phospholipase A2 and autotaxin in nerve injury-induced neuropathic pain. *J. Pharmacol. Exp. Ther.* **333**, 540–546.
- Milligan E. D. and Watkins L. R. (2009) Pathological and protective roles of glia in chronic pain. *Nat. Rev.* **10**, 23–36.
- Minoru N., Takuya Y., Mayumi N., Michiko N., Mayumi M., Tomoe T., Yoshinori Y. and Tsutomu S. (2006) Direct evidence for spinal cord microglia in the development of a neuropathic pain-like state in mice. *J. Neurochem.* **97**, 1337–1348.
- Moller T., Contos J. J., Musante D. B., Chun J. and Ransom B. R. (2001) Expression and function of lysophosphatidic acid receptors in cultured rodent microglial cells. *J. Biol. Chem.* **276**, 25946–25952.
- Piao Z. G., Cho I.-H., Park C. K. et al. (2006) Activation of glia and microglial p38 MAPK in medullary dorsal horn contributes to

- tactile hypersensitivity following trigeminal sensory nerve injury. *Pain* **121**, 219–231.
- Raghavendra V., Tanga F. and DeLeo J. A. (2003) Inhibition of microglial activation attenuates the development but not existing hypersensitivity in a rat model of neuropathy. *J. Pharmacol. Exp. Ther.* **306**, 624–630.
- Rashid M. H., Inoue M., Kondo S., Kawashima T., Bakoshi S. and Ueda H. (2003) Novel expression of vanilloid receptor 1 on capsaicin-insensitive fibers accounts for the analgesic effect of capsaicin cream in neuropathic pain. *J. Pharmacol. Exp. Ther.* **304**, 940–948.
- Rock R. B., Gekker G., Hu S., Sheng W. S., Cheeran M., Lokensgard J. R. and Peterson P. K. (2004) Role of Microglia in Central Nervous System Infections. *Clin. Microbiol. Rev.* **17**, 942–964.
- Romero-Sandoval A., Chai N., Natile-McMenemy N. and DeLeo J. A. (2008) A comparison of spinal Iba1 and GFAP expression in rodent models of acute and chronic pain. *Brain Res.* **1219**, 116–126.
- Roy A., Fung Y. K., Liu X. and Pahan K. (2006) Up-regulation of microglial CD11b expression by nitric oxide. *J. Biol. Chem.* **281**, 14971–14980.
- Schilling T., Repp H., Richter H., Koschinski A., Heinemann U., Dreyer F. and Eder C. (2002) Lysophospholipids induce membrane hyperpolarization in microglia by activation of IKCa1 Ca²⁺-dependent K⁺ channels. *Neuroscience* **109**, 827–835.
- Schilling T., Stock C., Schwab A. and Eder C. (2004) Functional importance of Ca²⁺-activated K⁺ channels for lysophosphatidic acid-induced microglial migration. *Eur. J. Neurosci.* **19**, 1469–1474.
- Scholz J. and Woolf C. J. (2002) Can we conquer pain? *Nat. Neurosci.* **5**(Suppl), 1062–1067.
- Scholz J. and Woolf C. J. (2007) The neuropathic pain triad: neurons, immune cells and glia. *Nat. Neurosci.* **10**, 1361–1368.
- Smani T., Zakharov S. I., Leno E., Csutora P., Trepakova E. S. and Bolotina V. M. (2003) Ca²⁺-independent phospholipase A2 is a novel determinant of store-operated Ca²⁺ entry. *J. Biol. Chem.* **278**, 11909–11915.
- Suter M. R., Wen Y. R., Decosterd I. and Ji R. R. (2007) Do glial cells control pain? *Neuron Glia Biol.* **3**, 255–268.
- Tanga F. Y., Raghavendra V. and DeLeo J. A. (2004) Quantitative real-time RT-PCR assessment of spinal microglial and astrocytic activation markers in a rat model of neuropathic pain. *Neurochem. Int.* **45**, 397–407.
- Tawfik V. L., Natile-McMenemy N., LaCroix-Fralish M. L. and DeLeo J. A. (2007) Efficacy of propentofylline, a glial modulating agent, on existing mechanical allodynia following peripheral nerve injury. *Brain Behav. Immun.* **21**, 238–246.
- Tikka T. M. and Koistinaho J. E. (2001) Minocycline provides neuroprotection against N-Methyl-D-aspartate neurotoxicity by inhibiting microglia. *J. Immunol.* **166**, 7527–7533.
- Tikka T., Fiebich B. L., Goldsteins G., Keinänen R. and Koistinaho J. (2001) Minocycline, a tetracycline derivative, is neuroprotective against excitotoxicity by inhibiting activation and proliferation of microglia. *J. Neurosci.* **21**, 2580–2588.
- Uchida H., Ma L. and Ueda H. (2010a) Epigenetic gene silencing underlies C-fiber dysfunctions in neuropathic pain. *J. Neurosci.* **30**, 4806–4814.
- Uchida H., Sasaki K., Ma L. and Ueda H. (2010b) Neuron-restrictive silencer factor causes epigenetic silencing of Kv4.3 gene after peripheral nerve injury. *Neuroscience* **166**, 1–4.
- Ueda H. (2006) Molecular mechanisms of neuropathic pain-phenotypic switch and initiation mechanisms. *Pharmacol. Ther.* **109**, 57–77.
- Ueda H. (2008) Peripheral mechanisms of neuropathic pain – involvement of lysophosphatidic acid receptor-mediated demyelination. *Mol. Pain* **4**, 11.
- Watkins L. R., Milligan E. D. and Maier S. F. (2001) Glial activation: a driving force for pathological pain. *Trends Neurosci.* **24**, 450–455.
- Woolf C. J. and Salter M. W. (2000) Neuronal plasticity: increasing the gain in pain. *Science (New York, NY)* **288**, 1765–1769.
- Wu D. C., Jackson-Lewis V., Vila M., Tieu K., Teismann P., Vadseth C., Choi D.-K., Ischiropoulos H. and Przedborski S. (2002) Blockade of microglial activation is neuroprotective in the 1-methyl-4-phenyl-1,2,3,6-tetrahydropyridine mouse model of Parkinson disease. *J. Neurosci.* **22**, 1763–1771.
- Yrjänheikki J., Keinänen R., Pellikka M., Hökfelt T. and Koistinaho J. (1998) Tetracyclines inhibit microglial activation and are neuroprotective in global brain ischemia. *Proc. Natl Acad. Sci. USA* **95**, 15769–15774.
- Zhang J. and De Koninck Y. (2006) Spatial and temporal relationship between monocyte chemoattractant protein-1 expression and spinal glial activation following peripheral nerve injury. *J. Neurochem.* **97**, 772–783.
- Zhao P., Waxman S. G. and Hains B. C. (2007) Extracellular signal-regulated kinase-regulated microglia-neuron signaling by prostaglandin E2 contributes to pain after spinal cord injury. *J. Neurosci.* **27**, 2357–2368.
- Zhuang Z.-Y., Wen Y.-R., Zhang D.-R., Borsello T., Bonny C., Strichartz G. R., Decosterd I. and Ji R.-R. (2006) A peptide c-Jun N-terminal kinase (JNK) inhibitor blocks mechanical allodynia after spinal nerve ligation: respective roles of JNK activation in primary sensory neurons and spinal astrocytes for neuropathic pain development and maintenance. *J. Neurosci.* **26**, 3551–3560.
- Zhuang Z. Y., Kawasaki Y., Tan P. H., Wen Y. R., Huang J. and Ji R. R. (2007) Role of the CX3CR1/p38 MAPK pathway in spinal microglia for the development of neuropathic pain following nerve injury-induced cleavage of fractalkine. *Brain Behav. Immun.* **21**, 642–651.

特集

抗がん剤誘発末梢神経障害の発生機序とその対処

動物実験からみたパクリタキセル誘発性末梢神経障害

植田睦美 植田弘師

長崎大学大学院医歯薬学総合研究科分子薬理学分野

ペインクリニック

Vol.31 No.7 (2010.7) 別刷

真興交易(株)医書出版部

動物実験からみたパクリタキセル誘発性末梢神経障害

植田睦美 植田弘師

長崎大学大学院医歯薬学総合研究科分子薬理学分野

要 旨

タキサン系製剤, ビンカルカロイド製剤, 白金製剤などの薬物は高い確率で末梢神経障害としての異常痛を誘発する。本稿では, 厚生労働省の推進する「予測・予防型」の安全対策という視点に立ち, この中毒性疼痛の性格づけ研究の解説を試みた。独自の解析方法では, C線維刺激に対する応答に変化はなく, A線維応答に限られていたが顕著な脱髄は認められなかった。むしろ, A線維に新たなカルシウムチャンネル $Ca\alpha_2\delta-1$ サブユニットの高発現が認められ, 実際, このサブユニットを標的とするガバペンチンが有効な疼痛抑制効果を示した。

(ペインクリニック 31: 885-892, 2010)

キーワード: パクリタキセル, 末梢神経障害, ガバペンチン

はじめに

日本人の病気による死亡原因の第1位である「がん」は, 飛躍的な医療分野の進歩と集学的医療チームの取り組みにより, もはや, 不治の病ではなくなってきた。手術, 放射線療法とともに, がんの主な治療方法として用いられてきた化学療法においても, 薬物の開発および剤型の開発により, 標的となるがん細胞に選択的に働きかけることができるようになり, 細胞毒性のより効果的な発現, また, 副作用の軽減に貢献している。しかし, 薬物の開発により, 新たな副作用も出てきている。従来, 抗がん剤の副作用は, 用いる薬物に限らず, 吐き気や倦怠感といったものが起こることが知られているが, 最近では, 薬物(タキサン系製剤, ビンカルカロイド製剤, 白金製剤)特異的に起こる「末梢神経障害」について, その作用機序が明

らかとなっていないことから, 有効な治療法がなく, 闘病生活のQOLを著しく低下させている。がん患者の7割に治療を必要とする痛みがあることはよく知られているが, この事実は, 抗がん剤が中毒性の神経障害性疼痛を誘発するという皮肉な現実を示している。卵巣がん, 非小細胞肺癌, 乳がん, 胃がんに適用を持つタキサン系化学療法製剤パクリタキセル(タキソール®)は, 同じく細胞内微小管ダイナミクス阻害作用を持つビンクリスチン(オンコピン®), およびDNA合成阻害作用を持つシスプラチン(ランダ®, プリプラチン®)とともに, 用量規制神経毒性(dose-limiting neurotoxicity)があるとされる¹⁻⁴⁾。その毒作用発現は1回投与量と総投与量に相関し, 手指のしびれ感, 四肢遠位部等における灼熱性感覚, 全感覚に及ぶ感覚障害, 腱反射消失, 感覚性運動失調, 自律神経症状などの末梢神経症状(感覚性ニューロパチー)として高頻度に観察される。しかし,

〈Special Article〉 Chemotherapy-induced peripheral neuropathy: Mechanisms and management

The mechanism of paclitaxel-induced peripheral neuropathic pain from the analyses of mice model

Mutsumi Ueda, et al

Division of Molecular Pharmacology and Neuroscience, Nagasaki University Graduate School of Biomedical Sciences

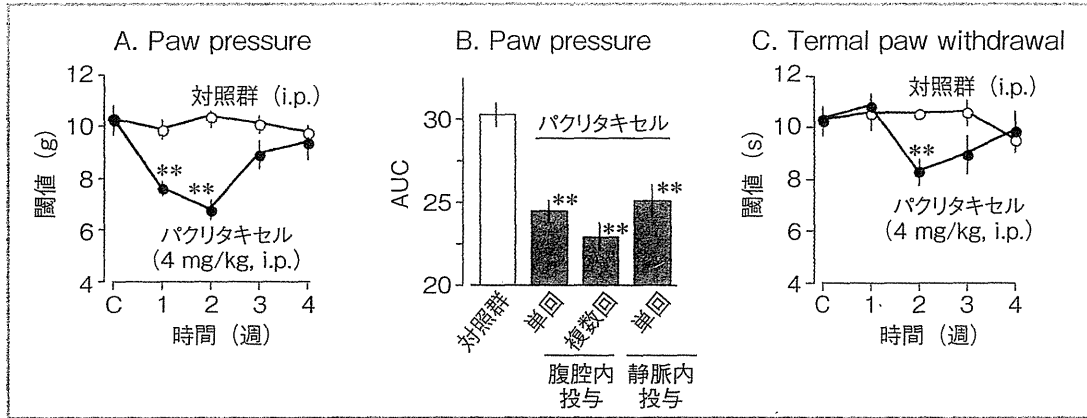


図1 パクリタキセル誘発性神経障害性疼痛

筋力低下は軽度である。高用量で使用した場合は、初回投与後1~3日程度で発症することがある。厚生労働省では、「末梢神経障害」を重篤副作用として位置づけ、医薬品の使用により発生する副作用疾患に着目した対策整備を行うとともに、副作用発生機序解明研究等を推進することにより、「予測・予防型」の安全対策への転換を図ることを目的として、平成17年度から「重篤副作用総合対策事業」をスタートさせた。本稿ではこの副作用としての感覚性ニューロパシー、特にパクリタキセル誘発性神経障害性疼痛について、動物実験モデルでの性格付けやガバペンチン（ガバベン®）による治療効果とその作用機構について解析を試みたい。

1. パクリタキセル誘発性神経障害性疼痛

パクリタキセルは、非小胞性肺がんの治療薬として、世界中で広く用いられている^{5,6)}。そのメカニズムは、細胞内の微小管重合の安定性を増し、脱重合を阻害することで、腫瘍細胞の分裂を阻害することによって考えられている^{7,8)}。しかし、パクリタキセルには中毒性の神経障害性疼痛を高頻度に誘発させることが知られ、その使用に制約がある。誘発される神経

障害性疼痛の分子メカニズムはまだ解明されておらず、その治療法も確立されていない。著者らは、パクリタキセル誘発性神経障害性疼痛の作用機序を見出すため、実験的モデルマウスの作成を試みた。パクリタキセル4mg/kgを雄ddYマウス腹腔内、静脈内に単回投与、腹腔内に隔日4回投与（days: 0, 2, 4, 6）し、投与直前から4週間、各種侵害試験の閾値の変化を評価した。観察中、腹水、体重減少、脱毛など他の重篤な副作用は見られなかった。パクリタキセル4mg/kg単回投与では、投与1週間後および2週間後において、機械触覚性刺激に対する閾値の低下、すなわちアロディニア現象が認められ、4週間後通常レベルに回復した⁹⁾（図1A）。機械触覚性刺激に対する閾値の低下は、投与部位、投与回数に関わらず見られた（図1B）。また、熱性刺激に対する痛覚閾値についても、パクリタキセル腹腔内単回投与において、2週間後で閾値低下が認められた（図1C）。これまでの報告では、パクリタキセル誘発性神経障害性疼痛モデルは、連続あるいは隔日の複数回投与、または単回の高用量投与されたものであった^{1,8,10-12)}ことを考えると、著者らのパクリタキセル4mg/kgの腹腔内単回投与方法は、より簡易でより臨床に近い方法であるといえるであろう。

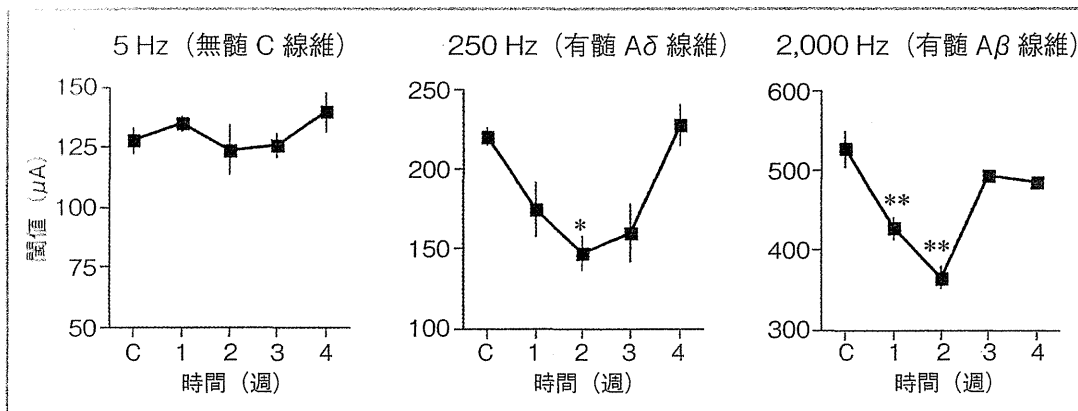


図2 パクリタキセル投与後の知覚神経線維の過敏応答 (EPW 試験法)

過敏応答を誘発することが示唆された。

2. 有髄 A 線維特異性の痛覚過敏

ニューロメーター®法は、複合性局所疼痛症候群 (complex regional pain syndrome) や、糖尿病等の一般的な疾患を起因とした他の末梢神経障害性疼痛において、ヒトでの知覚機能の評価に、临床上、広く用いられている^{13,14)}。ニューロメーター®を用いた経皮的電気刺激では、5, 250, 2,000 Hzの周波数ごとにそれぞれ無髄C, 有髄Aδ, 有髄Aβ線維が選択的に刺激されることが知られている^{14,15)}。この原理を利用して、独自に開発した知覚線維選択的解析法 (electrical stimulation-induced paw withdrawal: EPW 試験法) によりパクリタキセル誘発性痛覚過敏に関与する知覚線維について詳細な解析を行った^{12,16)}。ここでは、マウス右後肢に電極を当て、徐々に電流を強くし、パクリタキセル投与直前から4週間、閾値の変化を観察した (図2A)。パクリタキセル腹腔内単回投与後1, 2週間後にみられた250 Hz (有髄Aδ線維) と2,000 Hz (有髄Aβ線維) 刺激における閾値の低下は、4週間後には消失した。5 Hz (無髄C線維) 刺激には、何ら変化はみられなかった。これらのことから、パクリタキセルは、有髄Aδ, 有髄Aβ線維に特異的に

3. A 線維における $Ca\alpha_2\delta-1$ 発現上昇

パクリタキセル誘発性神経障害性疼痛が、有髄A線維機能亢進を示すことから、神経機能興奮に関与することの知られる電位依存性カルシウムチャンネル $\alpha_2\delta-1$ サブユニット ($Ca\alpha_2\delta-1$) の発現について解析した。このサブユニットは、カルシウムチャンネルポアを形成する α_1 サブユニットに会合することでチャンネル機能の亢進に寄与しており、特に神経終末部位においてサブスタンスP, CGRP, グルタミン酸などの神経伝達物質の遊離亢進に関わる^{17,18)}。まず、パクリタキセル投与後、3, 7, 14日後にL₄₋₆の脊髄後根神経節 (dorsal root ganglion: DRG) を採取し、 $Ca\alpha_2\delta-1$ mRNA をRT-PCR法で定量的解析を行った。 $Ca\alpha_2\delta-1$ mRNA の発現は、パクリタキセル投与3日後でわずかだが上昇し始め、7日後で最大となり、14日後にはコントロールレベルまでに戻った (図3A)。

つぎに、パクリタキセル投与後、7, 14, 28日後にL₄₋₆のDRGを採取し、 $Ca\alpha_2\delta-1$ 蛋白質をウエスタンブロット法で定量的解析を行った。 $Ca\alpha_2\delta-1$ 蛋白質は、パクリタキセル投与7日後には明らかに発現が上昇しており、14日後

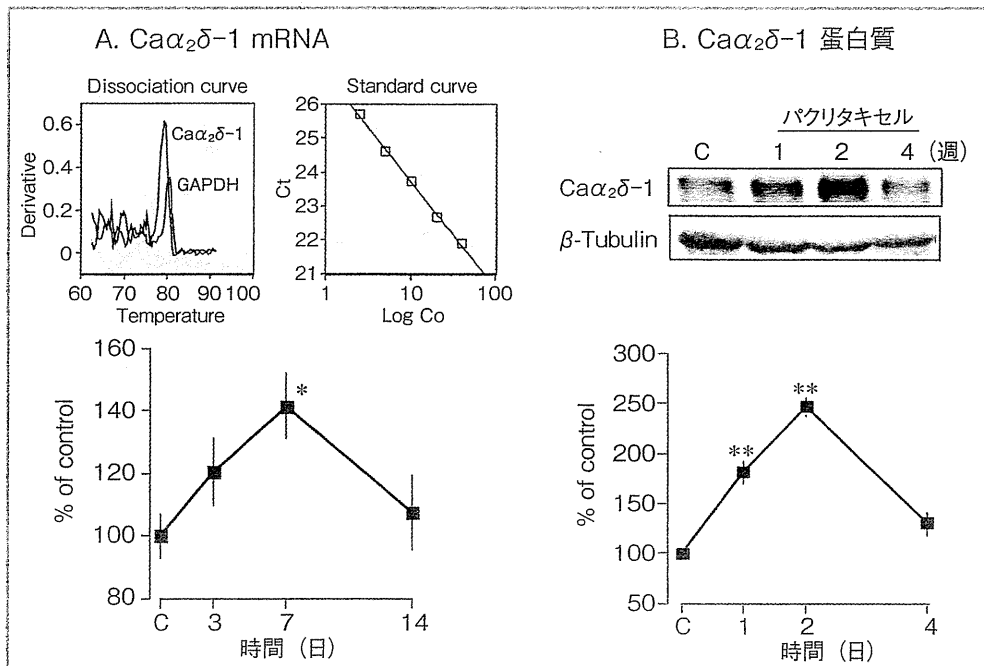


図3 パクリタキセル投与後のDRGにおけるCaα₂δ-1発現の時間経過

には、通常のDRGにおけるCaα₂δ-1蛋白質の2.5倍の発現上昇が認められた(図3B)。

さらに、パクリタキセル投与14日後のDRGにおけるCaα₂δ-1蛋白質の発現を免疫組織化学法により解析した。Vehicle処置群では、Caα₂δ-1蛋白質の発現は、主に、小径DRG神経細胞に局在しているが(図4A)、パクリタキセル処置群では、小径のみならず、中径/大径のDRG神経細胞(有髄A線維)にも見られた(図4A)。Vehicle処置群と比較して、パクリタキセル処置群では、Caα₂δ-1蛋白質陽性神経細胞が増加していた(図4B)。さらに、Vehicle処置群とパクリタキセル処置群において、Caα₂δ-1蛋白質陽性神経細胞数は、小型神経細胞ではほとんど変化はなかったが、中型/大型神経細胞においてはパクリタキセル処置群で顕著な増加がみられた(図4B)。

4. ガバペンチンによる疼痛治療効果

ガバペンチン(ガバペン®)は、近年、日本で承認された神経障害性疼痛治療薬であり、帯状疱疹後神経障害性疼痛や糖尿病性神経障害性疼痛に使用される。ガバペンチンの作用部位については、その構造がGABA(γ-aminobutyric acid)に類似することからGABAに関する作用であるのか、あるいはCaα₂δ-1に対する結合によるのか議論的となった¹⁰⁾が、2006年、遺伝学的な実験アプローチによりCaα₂δ-1に結合するという事実が確認された¹⁹⁾。この報告では、α₂サブユニット217番目アルギニンのアミノ酸変異マウスを用いることで、ガバペンチンやプレガバリンの結合が阻害されることが明らかにされた。慢性疼痛抑制に関しては、ガバペンチン(ガバペン®)が神経障害性疼痛、および末梢神経結紮や糖尿病性神経障害性疼痛

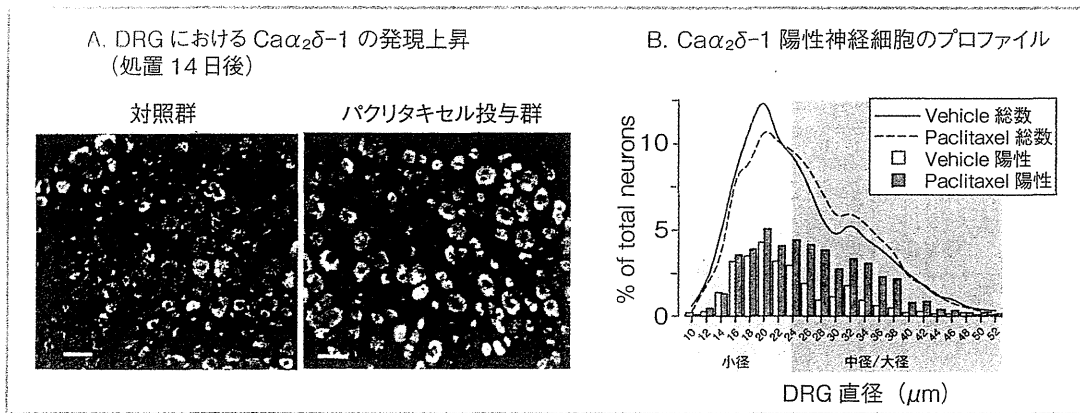


図4 A線維におけるCa $\alpha_2\delta$ -1の発現上昇

といった神経障害性疼痛動物モデルにおいて効果があること、熱性刺激痛覚過敏や機械的アロディニアを阻害することが明らかにされている²⁰⁻²⁴⁾。

著者等は、マウスにおけるパクリタキセル誘発性モデルのDRGにおいてCa $\alpha_2\delta$ -1発現上昇が認められたことから、ガバペンチンによる鎮痛効果を解析した。まず、パクリタキセル誘発神経障害性疼痛に対するガバペンチンの効果を観察するため、パクリタキセル投与2週間後、侵害行動実験の30分前に、ガバペンチンを腹腔内投与した。図5Aにみられるように、パクリタキセル誘発神経因性疼痛は、用量依存的に抑制され、ガバペンチン30mg/kg単独投与では、正常域にまで回復した。この疼痛抑制効果は、機械的アロディニアと熱性刺激痛覚過敏に対してともに観察された。また、有意な疼痛抑制効果は投与後24時間でも観察された(図5B)ことから、薬物の安定性だけでは説明できず、痛みの悪循環に対する抑制効果が関与すると考えられた。また、先にパクリタキセルによる疼痛過敏応答がA線維特異的であることを述べたが、ガバペンチン(30mg/kg; i. p.)はニューロメーター[®]を用いたEPW試験法における有髄A δ 、有髄A β 線維性のパクリタキセル誘発性痛覚過敏を完全に抑制した(図5C)。

まとめ

細胞内微小管重合安定化作用による抗がん活性を有する化学療法剤パクリタキセルが末梢神経性の神経障害性疼痛を誘発するという事実は薬物治療のコンプライアンスの面で大きな課題である。ビンカアルカロイドであるビンクリスチンは微小管重合を抑制し、抗がん活性を有するが、この薬物によっても同様な神経障害性疼痛が報告されている。こうした微小管重合のダイナミクスを阻害する薬物に共通して感覚性障害が選択的に認められるという事実は、中毒性神経障害性疼痛誘発活性の有無が、「予測・予防型」副作用対策上重要な検査項目たり得ることを示してきた。しかしその合理性については十分な証拠は示されていない。知覚神経は手足末端から脊髄までの長い軸索を有し、微小管重合抑制の影響をより受けやすいという説明もなされるが、同じ知覚神経でもC線維機能の活性に影響が見られなかったこと、運動神経系に顕著な影響が観察されなかったことから、必ずしもこの考え方は正しいとは言えない。幾つかの論文では、パクリタキセルで誘発される脊髄後角におけるCa $\alpha_2\delta$ -1発現上昇の方が重要であるということが述べられている^{11,25)}。興味があ

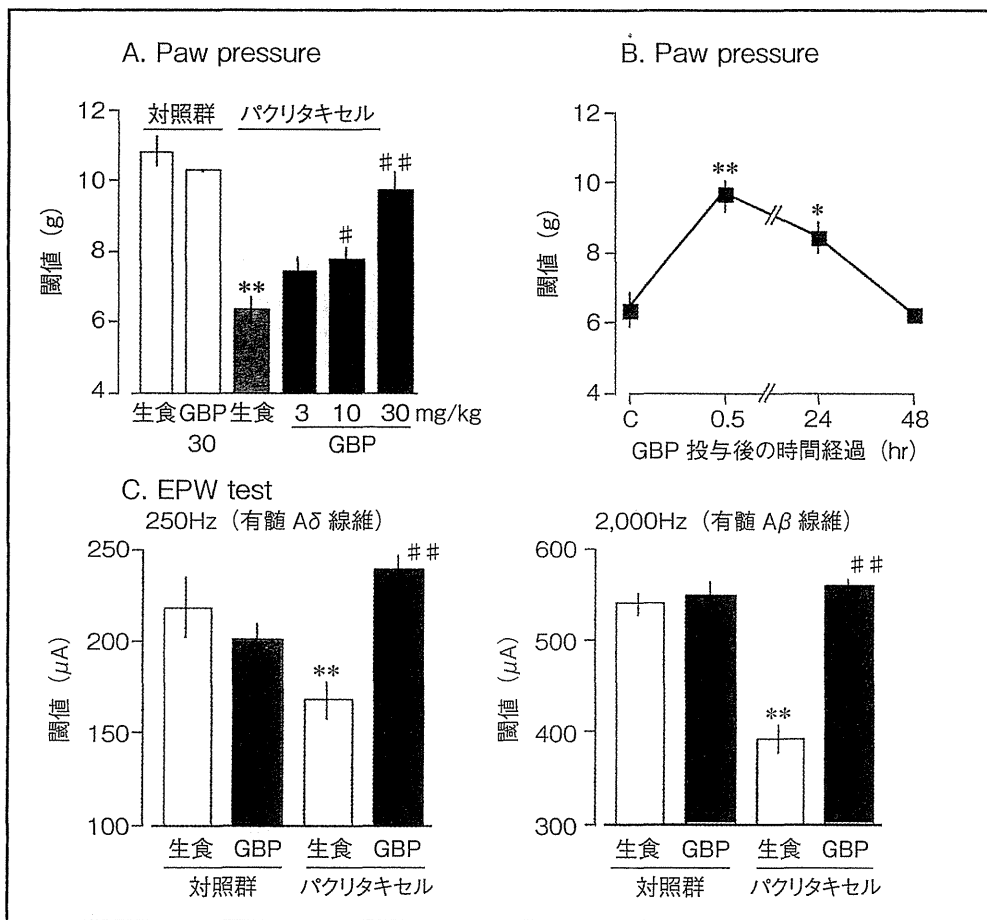


図5 パクリタキセル誘発性アロディニアに対するガバペンチンの鎮痛効果

るのは、DNA合成阻害による抗がん作用を有する白金製剤（シスプラチン等）にも神経障害性疼痛様症状が観察されることである^{26,27}。治療薬としてガバペンチンが有効であるという知見はDRGにおけるCa $\alpha_2\delta$ -1発現上昇¹¹との関連で合理性が認められるが、重要な事実、白金製剤も同様にCa $\alpha_2\delta$ -1発現上昇を誘発し、ガバペンチンが白金製剤誘発性疼痛を抑制するという報告¹¹や、ビンクリスチン誘発性疼痛はDRGにおいてCa $\alpha_2\delta$ -1発現上昇を伴わないがガバペンチンにより有意に抑制されるといった知見に見られる²⁵。したがって、化学療

法剤-神経障害性疼痛-Ca $\alpha_2\delta$ -1発現上昇-ガバペンチン疼痛抑制という図式は必ずしも一直線ではないことは明らかである。著者らは、坐骨神経結紮モデルによる神経障害性疼痛では、リゾホスファチジン酸（LPA）が初発原因分子でありLPA₁受容体が関与することを遺伝子欠損マウスでの研究から明らかにしている。実際、このモデルにおいて観察されるCa $\alpha_2\delta$ -1発現上昇はLPA₁受容体遺伝子欠損マウスにおいて消失することを見出している。しかし、われわれのこれまでの研究では、パクリタキセル誘発性疼痛においてLPAが関与するという

確かな証拠はまだ得られていない。実際、パクリタキセル誘発性疼痛では、坐骨神経結紮モデルで観察されるような LPA_1 受容体を介する C 線維刺激応答低下は認められない。このように化学療法剤による神経障害性疼痛様作用の分子機構についてはほとんど明らかにされていないのが現状である。一般に副作用の分子機構には多くの研究者は興味を示さない傾向があるが、国策としての「予測・予防型」副作用対策が本格化するならば、こうした未解決の課題も解き明かされるのではないかと期待される。

文 献

- 1) Cavaletti G, Bogliun G, Marzorati L, et al: Peripheral neurotoxicity of taxol in patients previously treated with cisplatin. *Cancer* 75 : 1141-1150, 1995
- 2) Chaudhry V, Rowinsky EK, Sartorius SE, et al: Peripheral neuropathy from taxol and cisplatin combination chemotherapy: Clinical and electrophysiological studies. *Ann Neurol* 35 : 304-311, 1994
- 3) Forsyth PA, Balmaceda C, Peterson K, et al: Prospective study of paclitaxel-induced peripheral neuropathy with quantitative sensory testing. *J Neurooncol* 35 : 47-53, 1997
- 4) Rowinsky EK, Eisenhauer EA, Chaudhry V, et al: Clinical toxicities encountered with paclitaxel (taxol). *Semin Oncol* 20 (4 Suppl 3) : 1-15, 1993
- 5) Kohler DR, Goldspiel BR: Paclitaxel (taxol). *Pharmacotherapy* 14 : 3-34, 1994
- 6) Socinski MA: Single-agent paclitaxel in the treatment of advanced non-small cell lung cancer. *Oncologist* 4 : 408-416, 1999
- 7) Horwitz SB: Mechanism of action of taxol. *Trends Pharmacol Sci* 13 : 134-136, 1992
- 8) Schiff PB, Fant J, Horwitz SB: Promotion of microtubule assembly *in vitro* by taxol. *Nature* 277(5698) : 665-667, 1979
- 9) Matsumoto M, Inoue M, Hald A, et al: Inhibition of paclitaxel-induced A-fiber hypersensitization by gabapentin. *J Pharmacol Exp Ther* 318 : 735-740, 2006
- 10) Field MJ, Cox PJ, Stott E, et al: Identification of the $\alpha_2\delta$ -1 subunit of voltage-dependent calcium channels as a molecular target for pain mediating the analgesic actions of pregabalin. *Proc Natl Acad Sci USA* 103 : 17537-17542, 2006
- 11) Gauchan P, Andoh T, Ikeda K, et al: Mechanical allodynia induced by paclitaxel, oxaliplatin and vincristine: Different effectiveness of gabapentin and different expression of voltage-dependent calcium channel $\alpha_2\delta$ -1 subunit. *Biol Pharm Bull* 32 : 732-734, 2009
- 12) 植田弘師, 松本みさき: ニューロメーターを用いた新しい知覚線維選択的侵害受容評価法. *日本薬理学雑誌* 131 : 367-371, 2008
- 13) Katims JJ: Neuroselective current perception threshold quantitative sensory test. *Muscle Nerve* 20 : 1468-1469, 1997
- 14) Masson EA, Boulton AJ: The Neurometer: Validation and comparison with conventional tests for diabetic neuropathy. *Diabet Med* 8 (Spec No.) : S63-S66, 1991
- 15) Pitei DL, Watkins PJ, Stevens MJ, et al: The value of the Neurometer in assessing diabetic neuropathy by measurement of the current perception threshold. *Diabet Med* 11 : 872-876, 1994
- 16) Matsumoto M, Xie W, Ma L, et al: Pharmacological switch in A β -fiber stimulation-induced spinal transmission in mice with partial sciatic nerve injury. *Mol Pain* 4 : 25, 2008
- 17) Davies A, Hendrich J, Van Minh AT, et al: Functional biology of the $\alpha_2\delta$ subunits of voltage-gated calcium channels. *Trends Pharmacol Sci* 28 : 220-228, 2007
- 18) Dooley DJ, Taylor CP, Donevan S, et al: Ca^{2+} channel $\alpha_2\delta$ ligands: Novel modulators of neurotransmission. *Trends Pharmacol Sci* 28 : 75-82, 2007
- 19) Gee NS, Brown JP, Dissanayake VU, et al: The novel anticonvulsant drug, gabapentin (Neurontin), binds to the $\alpha_2\delta$ subunit of a calcium channel. *J Biol Chem* 271 : 5768-5776, 1996
- 20) Cesena RM, Calcutt NA: Gabapentin prevents hyperalgesia during the formalin test in diabetic rats. *Neurosci Lett* 262 : 101-104, 1999
- 21) Hunter JC, Gogas KR, Hedley LR, et al: The effect of novel anti-epileptic drugs in rat experimental models of acute and chronic pain. *Eur J Pharmacol* 324 : 153-160, 1997
- 22) Hwang JH, Yaksh TL: Effect of subarachnoid gabapentin on tactile-evoked allodynia in a surgically induced neuropathic pain model in

- the rat. *Reg Anesth* 22 : 249-256, 1997
- 23) Luo ZD, Calcutt NA, Higuera ES, et al: Injury type-specific calcium channel $\alpha_2\delta$ -1 subunit up-regulation in rat neuropathic pain models correlates with antiallodynic effects of gabapentin. *J Pharmacol Exp Ther* 303 : 1199-1205, 2002
- 24) Miki S, Yoshinaga N, Iwamoto T, et al: Antinociceptive effect of the novel compound OT-7100 in a diabetic neuropathy model. *Eur J Pharmacol* 430 : 229-234, 2001
- 25) Xiao W, Boroujerdi A, Bennett GJ, et al: Chemotherapy-evoked painful peripheral neuropathy: Analgesic effects of gabapentin and effects on expression of the $\alpha_2\delta$ type-1 calcium channel subunit. *Neuroscience* 144 : 714-720, 2007
- 26) Attal N, Bouhassira D, Gautron M, et al: Thermal hyperalgesia as a marker of oxaliplatin neurotoxicity: A prospective quantified sensory assessment study. *Pain* 144 : 245-252, 2009
- 27) Authier N, Gillet JP, Fialip J, et al: An animal model of nociceptive peripheral neuropathy following repeated cisplatin injections. *Exp Neurol* 182 : 12-20, 2003

※ ※ ※

シンポジウム 腫瘍関連痛の最前線を探る

化学療法に伴う神経因性疼痛メカニズム*

植田 弘 師 松本みさき†

はじめに

痛みは本来、生体に対する警告系としての機能を果たしているが、過剰で持続的な痛みは除去する必要がある。治療を必要とする痛みについて見ると、炎症性の痛み機構はかなり解明されてきており、炎症性メディエーターによる無髄C線維の感作によって生じ、抗炎症薬やモルヒネによって除痛されることが知られている。一方、神経の障害に伴う慢性痛(神経因性疼痛)は、これらの薬剤に対して抵抗性を示すことから、その分子機構は炎症性疼痛とは異なるものであることが推測される。事実、傷害性神経因性疼痛モデルは有髄A線維に特異的な過敏応答(機能亢進)および脱髄現象を示すことを、筆者等は見出している。さらに、神経因性疼痛の初発因子として、リゾホスファチジン酸(lysophosphatidic acid: LPA)を同定した。本稿では、これらの研究成果に続いて、化学療法剤治療に伴って発生する疼痛(化学療法剤誘発性神経因性疼痛)に関する研究を紹介したい。

神経傷害性神経因性疼痛における
有髄線維の機能変調

著者らは、Seltzerら¹⁾のモデルに従い、坐骨神経を1/2程度を結紮するという神経傷害を施して作製した坐骨神経部分結紮性(神経傷害性)神経因性疼痛モデルを用いて、基礎的研究を行っている。このモデルでは、長期的な熱性過敏応答ならびに機械触覚性刺激に対する過敏応答(アロディニア現象)が観察される²⁾。こう

Key words: Neuropathic pain, Lysophosphatidic acid, Paclitaxel, Demyelination

*The mechanism of chemotherapy-induced neuropathic pain
†長崎大学大学院医歯薬学総合研究科分子薬理学分野. Hiroshi Ueda, Misaki Matsumoto: Division of Molecular Pharmacology and Neuroscience, Nagasaki University Graduate School of Biomedical Sciences

した知覚受容は、伝導速度が遅く鈍痛(slow pain)に関与する無髄C線維、伝導速度が速く鋭い痛み(fast pain)に関与する有髄A δ 線維、触覚性受容を担う有髄A β 線維によって伝達されていることから、各種神経線維の変調を選択的に解析し病態責任線維を同定することは、分子機構の解明ならびに創薬の観点から重要な課題である。著者らは、こうした課題の解明を第1に考え、独自に開発した知覚線維選択的解析法(electrical stimulation-induced paw withdrawal: EPW試験法)により詳細な解析を行った^{3,4)}。この解析法は、5, 250, 2000 Hzの刺激周波数をもつ経皮的電気刺激によりそれぞれ無髄C、有髄A δ 、有髄A β 線維を選択的に刺激できるニューロメーター装置を利用したものである。通電ゲルを塗布した2本の刺激電極をそれぞれマウスの後肢足底と甲に固定し、そこへ刺激電流を変えて刺激し、マウスが屈曲性逃避応答を示す電流値を閾値として決定する。解析の結果、神経傷害群では、無髄C線維の反応鈍麻(機能低下)が認められたのに対して、有髄A δ 線維ならびに有髄A β 線維の著しい過敏応答(機能亢進)が見出された^{3,4)}。これらのことから、熱性過敏応答ならびにアロディニア現象などの痛覚閾値の低下に関連する線維は、機能亢進を示す有髄A線維であると推測された。実際に、神経傷害に伴って、さまざまな疼痛関連分子が有髄A線維に発現することが報告されており、著者らも、熱感受性イオンチャネルTRPV1⁵⁾、ブラジキニンB1受容体⁶⁾、電位依存性カルシウムチャネル $\alpha_2\delta$ -1サブユニット(Ca $\alpha_2\delta$ -1)⁷⁾(図1-A)の新規発現を見出している。これらの分子に対する阻害剤は鎮痛効果を有することが知られていることから、新たな疼痛関連分子の発現が有髄A線維の機能亢進に関わっていると考えられる。

有髄A線維における脱髄

有髄線維における脱髄現象は、原因不明の慢性疼痛